Polymer 54 (2013) 431–439

Contents lists available at SciVerse ScienceDirect

Polymer

journal homepage: www.elsevier.com/locate/polymer

Micellization of linear A-*b*-(B-*alt*-C)$_n$ multiblock terpolymers in A-selective solvents

Yu-Chieh Hsu [a], Ching-I Huang [a,*], Weihua Li [b,*], Feng Qiu [b], An-Chang Shi [c]

[a] *Institute of Polymer Science and Engineering, National Taiwan University, Taipei 10617, Taiwan*
[b] *Department of Macromolecular Science, Fudan University, Shanghai 200433, China*
[c] *Department of Physics and Astronomy, McMaster University, Hamilton, Ontario, Canada L8S 4M1*

ARTICLE INFO

Article history:
Received 21 September 2012
Received in revised form
31 October 2012
Accepted 2 November 2012
Available online 7 November 2012

Keywords:
Multicompartment micelles
Self-consistent field theory
Multiblock terpolymers

ABSTRACT

We used three-dimensional self-consistent field theory to investigate the micellization behavior of A-*b*-(B-*alt*-C)$_n$ multiblock terpolymers in the presence of a solvent that is selective to the terminal A-block. In particular, we focused on the effects of the incompatibility parameter between B and C, χ_{BC}, and the composition of the solvophilic A-block, f_A, on the formation of micelles from ABC triblock and A(BC)$_3$ multiblock terpolymers, respectively. We observed a general trend that a segmented packing of B- and C-layers along the axial direction of the micelles is favored than the coaxial packing with the increasing of χ_{BC} or decreasing of f_A. The separation of B and C blocks within a micelle leads to the formation of a variety of multicompartment micelle morphologies, such as core–shell–corona spherical micelles, hamburgers, and bump-surface micelles, in the ABC triblock copolymers. In the A(BC)$_3$ multiblock terpolymers, we discovered more fascinating micelles by implementing the SCFT simulation than by the DPD simulation. Besides the BC-segmented worm-like micelles, which have been found in the DPD simulation work, concentric multilayer spheres and vesicles can be formed by the solvent-induced effect when the solvophilic A-block is a majority component. The SCFT method provides an efficient way to screen promising molecular architectures for the ability to self-assemble into technologically promising hierarchical structures.

1. Introduction

The self-assembly of block copolymers is of great interest because of its intrinsic fascination to form rich ordered nanostructures [1–3], and the potential applications in a wide range of fields, such as nanolithography [4,5], drug delivery systems [6,7], and organic photovoltaics [8,9]. With the development of synthetic techniques, many copolymers with more than two types of monomers or with various kinds of chain topologies, such as linear, star, comb, and cyclic, have been successfully produced. This development enriches the formation of self-assembled morphologies on multiple length scales. Moreover, the addition of selective solvents to block copolymers also attracts intensive research attention, both experimentally and theoretically, as it opens the opportunity to engineer novel nano-particles with complex internal structures [2,3].

Compared with the simplest diblock copolymers, which can self-assemble into a rather limited number of ordered phases (lamella, cylinder, sphere, gyroid, and Fddd network phases) [10–12], ABC terpolymers exhibit much more complex self-assembling behavior [13–20]. For example, even in the simplest architecture of linear ABC triblock terpolymers, the morphologies are divided into two categories, nonfrustrated and frustrated phases, due to the topological constraint of the copolymers. Each of these categories includes a large number of complex phases [16,17]. Specifically, when the interaction between the two end blocks is larger than that between the middle and either end blocks ($\chi_{AC} >> \chi_{AB} \approx \chi_{BC}$), the morphologies are nonfrustrated [16], which are dominated by the strong incompatibility between A and C blocks. In the nonfrustrated case the system tends to form ordered structures with less AC interfaces, such as A-core/B-shell/C-matrix, C-core/B-shell/A-matrix, and alternating lamellae (A/B/C). On the contrary, when the interaction between the two end blocks is the smallest ($\chi_{AC} << \chi_{AB} \approx \chi_{BC}$), the morphologies are frustrated [17]. Because of the weak χ_{AC}, the C blocks tend to be in contact with the A-blocks. On the other hand, the topology of the ABC chain dictates that the B blocks have to be located between the A and C blocks. The

* Corresponding authors. Tel.: +886 2 33665886; fax: +886 2 33665237.
E-mail addresses: chingih@ntu.edu.tw (C.-I. Huang), weihuali@fudan.edu.cn (W. Li).

0032-3861/$ – see front matter © 2012 Elsevier Ltd. All rights reserved.
http://dx.doi.org/10.1016/j.polymer.2012.11.005

arrangement of the B blocks at the AC interfaces leads to a rich variety of hierarchical structure-within-structure phases, including cylinders in lamellae, spheres in lamellae, spheres on cylinders, rings on cylinders, and spheres on spheres. Recent interest has grown in a class of linear multiblock terpolymers containing one or two long end-blocks and multiple short mid-blocks [21–36]. In a pioneering experimental work, Masuda et al. [23] synthesized an undecablock terpolymer consisting of two long poly(2-vinylpyridine) (P) end-blocks and short polystyrene–polyisoprene (SI) alternating middle-blocks. The authors observed the formation of spheres-within-lamellae, cylinders-within-lamellae, parallel lamellae-within-lamellae morphology, coaxial cylinders, and concentric spheres structures. On the other hand, an asymmetric linear multiblock terpolymer CECEC-P (C: cyclohexylethylene, E: ethylene, P: propylene) with only one long end-block was synthesized and perpendicular lamellae-within-lamellae morphology was observed by Fleury and Bates [24,25]. Subsequent theoretical studies suggest that the formation of inner thin-layers is under the soft confinement of two thick layers of the end-blocks, and the number of thin-layers can be tuned through the interaction parameters and the relative length of the middle-blocks and the end-blocks [33–35]. Wang et al. [36] reported that for most interaction parameters between components i and j, χ_{ij}, the A-*block*-(B-*alt*-C) copolymers tend to self-assemble into parallel packed hierarchical structure-within-structures. One exception is when $\chi_{BC} >> \chi_{AB} > \chi_{AC}$, the segregated B and C small-length-scale domains are perpendicular to the large-length-scale morphologies.

In addition to the hierarchical structures in melts, ABC terpolymers have been shown to be excellent candidates for forming multicompartment and multicore micelles in which the two solvophobic blocks adopt distinct domains within the cores of the micelles. In a comparison between the linear ABC triblock and multiblock terpolymers in a selective solvent, there is an interesting question that how the multiblock feature influences the structure formation. Experimentally, there have been quite a number of studies that showed the linear ABC triblock terpolymers tend to form core–shell–corona micelles in solvents selective for one terminal block [37–45]. Besides, Erhardt et al. [46] and Liu et al. [47] reported the formation of Janus spheres and Janus cylinders in the linear ABC triblock copolymers solutions, where the two end-blocks A and C are solvophilic and the mid-block B is solvophobic. To the best of our knowledge, there exist only very few studies of exploring the micelles formed by the linear multiblock terpolymers [48–51]. For example, Thünemann et al. [49] have reported the formation of two-compartment cylindrical-shape micelles of C-core/B-shell/A-corona by ABCBA pentablock copolymers consisting of a hydrophilic block of poly(ethylene oxide) (A) and two hydrophobic blocks of poly(gamma-benzyl L-glutamate) (B) and poly(perfluoro ether) (C). Though these experimental studies have demonstrated a rich variety of interesting micelles that the linear triblock and multiblock terpolymers can form, obtaining a better understanding the effects of varying the number of the solvophobic B and C blocks on the micellization behavior from the experimental studies can be expensive and time consuming.

In contrast, computer simulation and theoretical calculation provide efficient tools to study the self-assembling behaviors of block copolymer systems [10,11,52–54], and thus to explore new structures in a larger parameter space. As a complementary method to computer simulations, the self-consistent field theory (SCFT) provides a powerful tool in the study of block copolymers [10,11,52]. For the cases of micelle formation, Wang et al. [55] and Ma and Jiang [56] used two-dimensional (2D) SCFT to investigate the phase behavior of micelles formed by ABC linear triblock copolymers in dilute solutions. By tuning the hydrophobic degree and its difference between B and C blocks, some typical micelles and various types of vesicles were obtained. Although the morphologies calculated by 2D SCFT are mostly corresponding to the micellar structures in 3D, it is difficult to explore more complex microstructures when the space is restricted in two-dimension. As the fast development of computer technology, full three-dimensional (3D) SCFT calculation is feasible, thus it becomes more powerful in the exploration of intricate 3D micelles. Up to now, Ma et al. [57] and Wang and Lin [58] have successfully applied 3D SCFT to investigate the self-assembly of linear ABC triblock terpolymers in dilute solutions. Ma et al. reported that the spherical, cylindrical, and discoidal micelles with bumpy surfaces could be formed via turning the solvent selectivity with respect to the solvophobic blocks A and B. Wang and Lin focused on the linear ABC terpolymers consisting of a solvophilic midblock (B) and two solvophobic end-blocks (A and C). In their results, a number of novel micelles were found, such as spheres with A and C helix-like cores, spheres with A and C disk-like cores, and cylinders with A and C ring-like cores. As for the multiblock copolymers in dilute solutions, Huang et al. [59] investigated micellar structures of the A_2-*star*-(B-*alt*-C) terpolymers using DPD simulation method. They discussed the formation of multicompartment micelles through controlling the repeat number of B/C blocks, the composition of solvophilic block A, the incompatibility between the two solvophobic B and C, and the difference of the incompatibility between the two solvophobic B and C with respect to the solvent. In addition to the typical micelles formed by ABC triblock copolymers, some fascinating multicompartment micelles were observed, including cores with helical B and C, coaxial bowl-like micelles, and BC segmented worm-like micelles. However, up to the present, one of the most obvious shortcomings in computer simulations has been the very limited monomer numbers, typically between 10 and 40 [18,32,53,59]. Therefore, to lessen the influence of the limited chain length, computer simulation methods usually focus on the strong-segregation region. It is worthy to note that the small number of monomers definitely reduces the effect of polymer configurational entropy, especially in the case of multiblock copolymers.

In this work, we used 3D real-space SCFT method to investigate the micelle formation of one type of linear multiblock terpolymers

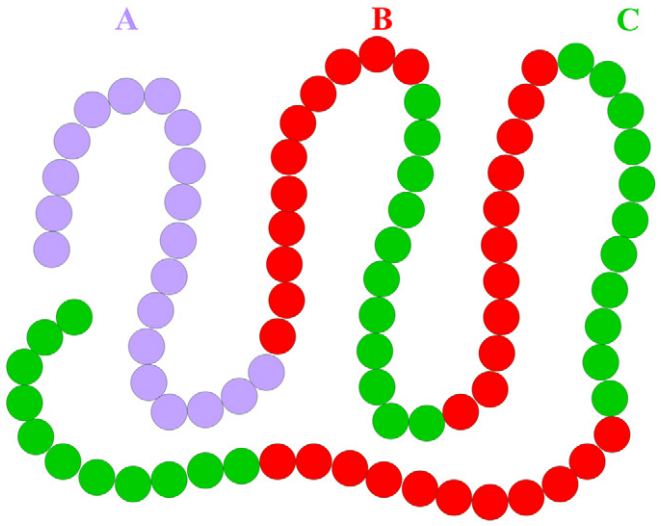

Fig. 1. A schematic plot of the model A-*b*-(B-*alt*-C)$_n$ multiblock terpolymer. A, B, and C blocks are shown in light purple, red, and green, respectively. (For interpretation of the references to color in this figure legend, the reader is referred to the web version of this article.)

A(BC)$_n$ in a selective solvent of S, where A block is solvophilic, and B and C blocks are solvophobic. The schematic plot of molecular structure of A-*b*-(B-*alt*-C)$_n$ multiblock terpolymers is displayed in Fig. 1, where A, B, and C blocks are labeled in light purple, red, and green, respectively, and n is the repeating number of B and C alternating blocks. In particular, we constructed and compared the morphology maps for $n = 1$ (the system was reduced to ABC triblock terpolymer) and 3 as a function of the molecular variables. In this way, the effects of multiple solvophobic blocks on the micellization behavior can be revealed.

2. Theoretical method

We consider a system of volume V containing monodisperse A-*b*-(B-*alt*-C)$_n$ multiblock terpolymers in the presence of a selective solvent S with average volume fractions of ϕ and $1-\phi$, respectively. The degree of polymerization of the terpolymer is N and the compositions of A, B, and C blocks are f_A, f_B, and f_C, respectively. The polymer chain is composed of n alternating B and C blocks, which are linked to one A block. Accordingly, the degree of polymerization of one B/C block is $N_{BC} = N(f_B + f_C)/n$ and the compositions of each B and C alternating blocks are $\Delta f_B = f_B/n$ and $\Delta f_C = f_C/n$, respectively.

We assume that the system is incompressible and each segment has the same statistical segment length of b. According to the mean-field theory based on the ideal Gaussian chain model, the free energy per chain is given by Eq. (1)

$$\frac{F}{k_BT} = -\phi\ln\left(\frac{Q_{CO}}{\phi}\right) - (1-\phi)N\ln\left(\frac{Q_S}{1-\phi}\right) + \frac{1}{V}\int d\vec{r}\begin{bmatrix}\chi_{AB}N\phi_A(\vec{r})\phi_B(\vec{r}) + \chi_{AC}N\phi_A(\vec{r})\phi_C(\vec{r}) + \chi_{BC}N\phi_B(\vec{r})\phi_C(\vec{r})\\ +\chi_{AS}N\phi_A(\vec{r})\phi_S(\vec{r}) + \chi_{BS}N\phi_B(\vec{r})\phi_S(\vec{r}) + \chi_{CS}N\phi_C(\vec{r})\phi_S(\vec{r})\\ -\omega_A(\vec{r})\phi_A(\vec{r}) - \omega_B(\vec{r})\phi_B(\vec{r}) - \omega_C(\vec{r})\phi_C(\vec{r}) - \omega_S(\vec{r})\phi_S(\vec{r})\\ -\xi(\vec{r})(1-\phi_A(\vec{r}) - \phi_B(\vec{r}) - \phi_C(\vec{r}) - \phi_S(\vec{r}))\end{bmatrix} \quad (1)$$

where T is the temperature, and k_B is the Boltzmann constant. $\phi_i(\vec{r})$ is the volume fraction of component i (i = A, B, C, and S), and $\omega_i(\vec{r})$ are the mean fields acting on component i (i = A, B, C, and S). χ_{ij} is the Flory–Huggins interaction parameter between components i and j (i, j = A, B, C, and S). $\xi(\vec{r})$ is a Lagrange multiplier that is used to ensure the incompressibility of the system. Q_{CO} and Q_S are the partition functions of a single copolymer chain and a solvent molecule, respectively, given by Eqs. (2) and (3)

$$Q_{CO} = \frac{1}{V}\int d\vec{r}\, q_{CO}(\vec{r}, 1) \quad (2)$$

$$Q_S = \frac{1}{V}\int d\vec{r}\exp\left(\frac{-\omega_S(\vec{r})}{N}\right) \quad (3)$$

The partition function of the terpolymer is in terms of propagators $q_{CO}(\vec{r}, s)$ and $q^+_{CO}(\vec{r}, s)$. The propagators $q_{CO}(\vec{r}, s)$ and $q^+_{CO}(\vec{r}, s)$ represent the probabilities to find the polymer segment of contour length s at space coordinates of $\vec{r}$ starting from two free ends, respectively. Both propagator functions satisfy the modified diffusion equations

$$\frac{\partial q_{CO}(\vec{r}, s)}{\partial s} = \frac{1}{6}Nb^2 q_{CO}(\vec{r}, s) - \omega_i(\vec{r})q_{CO}(\vec{r}, s) \quad (4)$$

$$\frac{\partial q^+_{CO}(\vec{r}, s)}{\partial s} = -\frac{1}{6}Nb^2 q^+_{CO}(\vec{r}, s) + \omega_i(\vec{r})q^+_{CO}(\vec{r}, s) \quad (5)$$

where the mean fields $\omega_i(\vec{r})$ are specified by ($0 \le i < n$)

$$\omega_i(\vec{r}) = \begin{cases}\omega_A(\vec{r}), 0 \le s < f_A\\ \omega_B(\vec{r}), f_A + i(\Delta f_B + \Delta f_C) \le s < f_A + i(\Delta f_B + \Delta f_C) + \Delta f_B\\ \omega_C(\vec{r}), f_A + i(\Delta f_B + \Delta f_C) + \Delta f_B \le s < f_A + (i+1)(\Delta f_B + \Delta f_C)\end{cases} \quad (6)$$

The initial conditions are $q_{CO}(\vec{r}, 0) = 1$ and $q^+_{CO}(\vec{r}, 1) = 1$ for Eqs. (4) and (5), respectively.

Minimization of the free energy specified in Eq. (1) with respect to the volume fraction functions and the mean fields leads to the following SCFT equations

$$\phi_A(\vec{r}) = \frac{\phi}{Q_{CO}}\int_0^{f_A} q_{CO}(\vec{r}, s)q^+_{CO}(\vec{r}, s)ds \quad (7)$$

$$\phi_B(\vec{r}) = \frac{\phi}{Q_{CO}}\sum_{i=0}^{n-1}\int_{f_A+i(\Delta f_B+\Delta f_C)}^{f_A+i(\Delta f_B+\Delta f_C)+\Delta f_B} q_{CO}(\vec{r}, s)q^+_{CO}(\vec{r}, s)ds \quad (8)$$

$$\phi_C(\vec{r}) = \frac{\phi}{Q_{CO}}\sum_{i=0}^{n-1}\int_{f_A+i(\Delta f_B+\Delta f_C)+\Delta f_B}^{f_A+(i+1)(\Delta f_B+\Delta f_C)} q_{CO}(\vec{r}, s)q^+_{CO}(\vec{r}, s)ds \quad (9)$$

$$\phi_S(\vec{r}) = \frac{1-\phi}{Q_S}\exp\left[\frac{-\omega_S(\vec{r})}{N}\right] \quad (10)$$

$$\omega_A(\vec{r}) = \chi_{AB}N\phi_B(\vec{r}) + \chi_{AC}N\phi_C(\vec{r}) + \chi_{AS}N\phi_S(\vec{r}) + \xi(\vec{r}) \quad (11)$$

$$\omega_B(\vec{r}) = \chi_{AB}N\phi_A(\vec{r}) + \chi_{BC}N\phi_C(\vec{r}) + \chi_{BS}N\phi_S(\vec{r}) + \xi(\vec{r}) \quad (12)$$

$$\omega_C(\vec{r}) = \chi_{AC}N\phi_A(\vec{r}) + \chi_{BC}N\phi_B(\vec{r}) + \chi_{CS}N\phi_S(\vec{r}) + \xi(\vec{r}) \quad (13)$$

$$\omega_S(\vec{r}) = \chi_{AS}N\phi_A(\vec{r}) + \chi_{BS}N\phi_B(\vec{r}) + \chi_{CS}N\phi_C(\vec{r}) + \xi(\vec{r}) \quad (14)$$

The volume fractions must satisfy the incompressibility condition of Eq. (15)

$$\phi_A(\vec{r}) + \phi_B(\vec{r}) + \phi_C(\vec{r}) + \phi_S(\vec{r}) = 1 \quad (15)$$

At present, there are a number of complementary numerical approaches to solve the modified diffusion equations of SCFT. The first one is the spectral method proposed by Matsen and Schick [10]. In the spectral method, all space functions are expressed in terms of a set of orthonormal basis functions according to a prior symmetry, and then solve the SCFT equations with respect to the

coefficients of these basis functions. The second approach is the real-space method proposed by Drolet and Fredrickson [60,61]. The third approach is pseudo-spectral method [62], which takes the advantage of switching between real and reciprocal spaces. As it solves the modified diffusion equation by the split-step fast Fourier transform, it provides a higher operating efficiency. In our studies we used the pseudo-spectral method.

We perform SCFT calculations in a cubic box that is discretized into a 64 × 64 × 64 lattice. Periodic boundary conditions are automatically imposed on each direction by the Fourier transition in the pseudo-spectral method. Each of our simulation results is repeated at least 10 times with different initial states to obtain the microstructures. It should be noted that two or more microstructures may be observed in our some simulations. In order to ensure which one is the most stable microstructure, we consider the individual microstructure to be the initial state. After recalculating them in the same parameters, we compare their free energies to identify the most stable microstructure. The iterating convergence of the SCFT salvation is determined by both the free energy and the incompressibility condition. The change of free energy is required to be less than 10^{-7} in a large number of iterations and the change of the incompressibility on each point is required to be smaller than 10^{-7}.

3. Results and discussion

In the present work, we examine how the multiblock feature affects the micellization behavior of ABC terpolymers. Because the number of parameter space of the present system is huge, it is impossible to explore the whole phase space. Instead, we will restrict our attention to a set of parameters representing typical cases encountered in experiments. First, we assume that the copolymer has a constant total degree of polymerization of $N = 120$, which we believe it is long enough to include the effect of polymer configurational entropy and has equal B and C blocks, $f_B N = f_C N$. With this assumption, the copolymer composition can be described by only one independent volume fraction of f_A. There are six interaction parameters χ_{ij} (i,j = A, B, C, and S) to measure the immiscibility between the four components. Then, we use the following conditions to reduce the number of independent interaction parameters: $\chi_{AS} = 0.27$, $\chi_{AB} = \chi_{AC} = 1.0$, and $\chi_{BS} = \chi_{CS} = 1.2$, except otherwise specified. The last parameter restriction is that the concentration of the copolymer to be fixed as dilute as $\phi = 0.1$. The above parameter reduction allows us to focus on the effects of the composition of solvophilic block, f_A, the incompatibility between B and C blocks, χ_{BC}, and the repeat number of B/C alternating blocks, n. For the reason of clarity, the morphologies in the solution system are plotted against the density profiles of A, B, and C blocks, and that of the solvent S is omitted.

When $n = 1$, the A-b-(B-*alt*-C)$_n$ multiblock terpolymer is reduced to an ABC triblock copolymer. The phase diagram with respect to χ_{BC} and f_A of ABC triblock terpolymer is shown in Fig. 2. Firstly, we observed BC-mixed spherical micelles or C-core/B-shell/A-corona spherical micelles for the various fractions of f_A in the region of low value χ_{BC}. When χ_{BC} increases to be intermediate or high value, a fascinating self-assembling behavior of micelles as increasing f_A can be observed. When the solvophilic block A is short ($f_A = 0.1$–0.3), the micelles of B–C–B hamburgers are formed in a large phase-region. It is because that B blocks are jointed to the A blocks, thus the most of A blocks are aggregated to the outside of B blocks. Therefore, most of B blocks can be isolated from the solvent. Nevertheless, without the screening of A blocks, C blocks are curled into the core, which is sandwiched by the two ends of B blocks. This morphology can minimize the contacting surfaces of B/C blocks to the solvents. Similarly, Zhu et al. [53] also reported the formation of hamburger micelles when the solvophilic block is short and the incompatibility degrees between the different blocks are strong. However, when decreasing the incompatibility parameters between the blocks, they observed the formation of vesicles instead of the core–shell–corona spheres. This is reasonable mainly due to

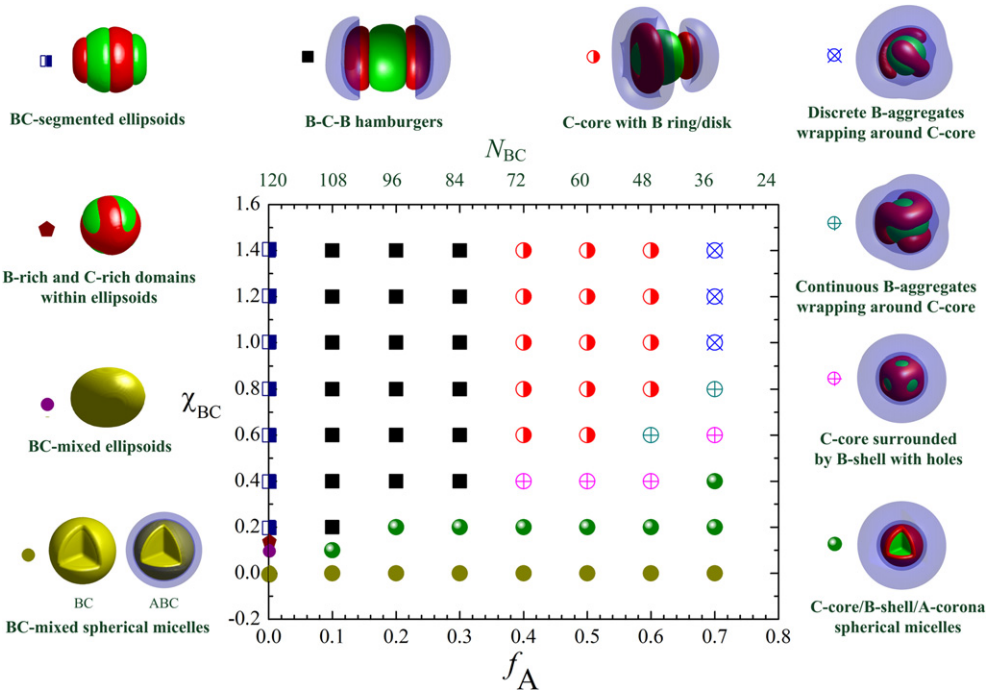

Fig. 2. The phase diagram of ABC linear triblock terpolymers in dilute solutions in terms of χ_{BC} and f_A when $N = 120$, $\phi = 0.1$, $\chi_{AB} = \chi_{AC} = 1.0$, $\chi_{AS} = 0.27$, and $\chi_{BS} = \chi_{CS} = 1.2$. In each representative micelle, A, B, and C blocks are shown in light purple, red, and green, respectively. The BC-mixed is labeled as yellow. (For interpretation of the references to color in this figure legend, the reader is referred to the web version of this article.)

the fact that their simulated triblock chains are very short, which favors the formation of vesicles. Next, when the solvophilic block A increases to be equal or larger than solvophobic blocks (B + C), the formed micelles are similar to B–C–B hamburgers except that the disk-like structure is transferred to ring-like structure on one side of B block while keeping the other side of B block the disk-form. The formed micelles are referred as "C core with B ring/disk". In this micelle, the interface between the C core and the solvent is reduced by the formation of ring-like B-end cap. It is obvious that the orientation of C core with B ring/disk micelles in the small-length scale domain is an intermediate transition between radial direction (–core–shell-corona type micelles) and axial direction (hamburger micelles) along with the shape of micelles. Finally, when the solvophilic block A is the majority (f_A = 0.7), the morphology of micelles tends to be core–shell–corona type micelles, as have been observed in experiments [37–39]. In more detail, we observe an interesting variation of core–shell–corona type micelles with the increasing of the interaction parameter χ_{BC}. As clearly seen in Fig. 2, when χ_{BC} increases to an intermediate value about 0.6, though the formed micelles are still C core-B shell-A corona spheres, there exist some holes in the B shell. As χ_{BC} parameter increases further, the B domains are transferred to be continuous B-aggregates, which are surrounded in the surface of C core. When χ_{BC} keeps increasing, the continuous B-aggregates are broken to be the discrete B-aggregates, which are randomly bumped in the surface of C core. These bump-surface core–shell–corona type micelles are because of the increasing degree of the B and C segregation toward the axial direction of the micelles as χ_{BC} increases. Up to the present, most of the theoretical researches are not focused on the variations of micelles when the solvophilic A block is the majority component, as in our study.

In the limited conditions of $f_A = 0$, the ABC triblock copolymer is reduced to the simple symmetric BC diblock copolymer. Here, we systematically explored the variations of microstructures as χ_{BC} increases in this specific situation of $f_A = 0$. A series of morphology

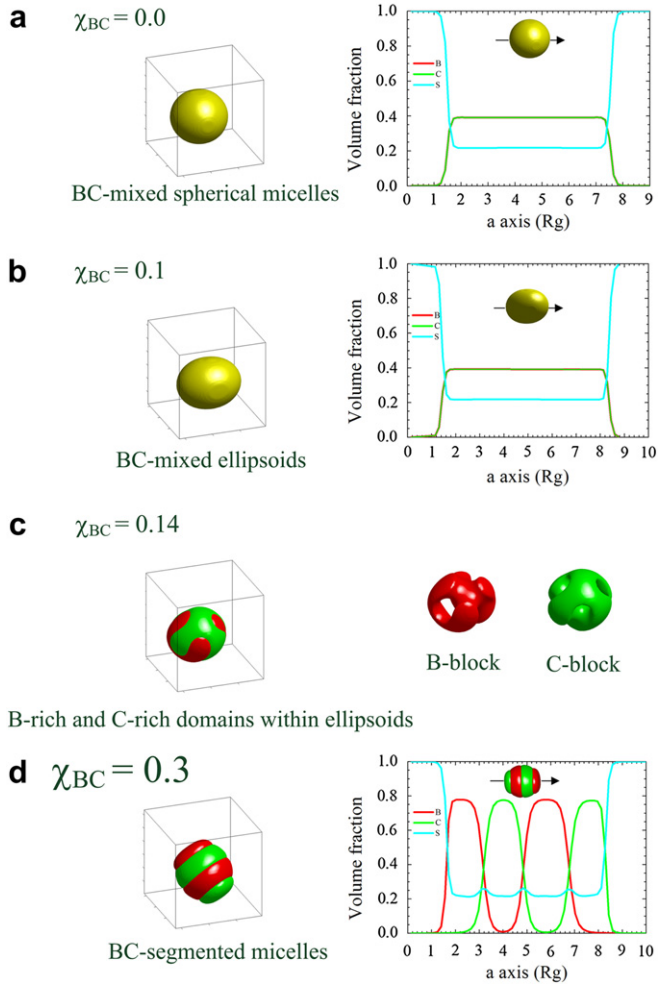

Fig. 3. Simulated micelle patterns and corresponding volume fraction profiles of B, C, and solvent S for BC diblock copolymers in a poor solvent with N = 120, ϕ = 0.1, $\chi_{BS} = \chi_{CS}$ = 1.2, and χ_{BC} equal to (a) 0.0, (b) 0.1, (c) 0.14, and (d) 0.3, respectively. In each representative of microstructures, B and C blocks are shown in light purple and green, respectively, and the solvent S is omitted for clarity. The BC-mixed is labeled as yellow. (For interpretation of the references to color in this figure legend, the reader is referred to the web version of this article.)

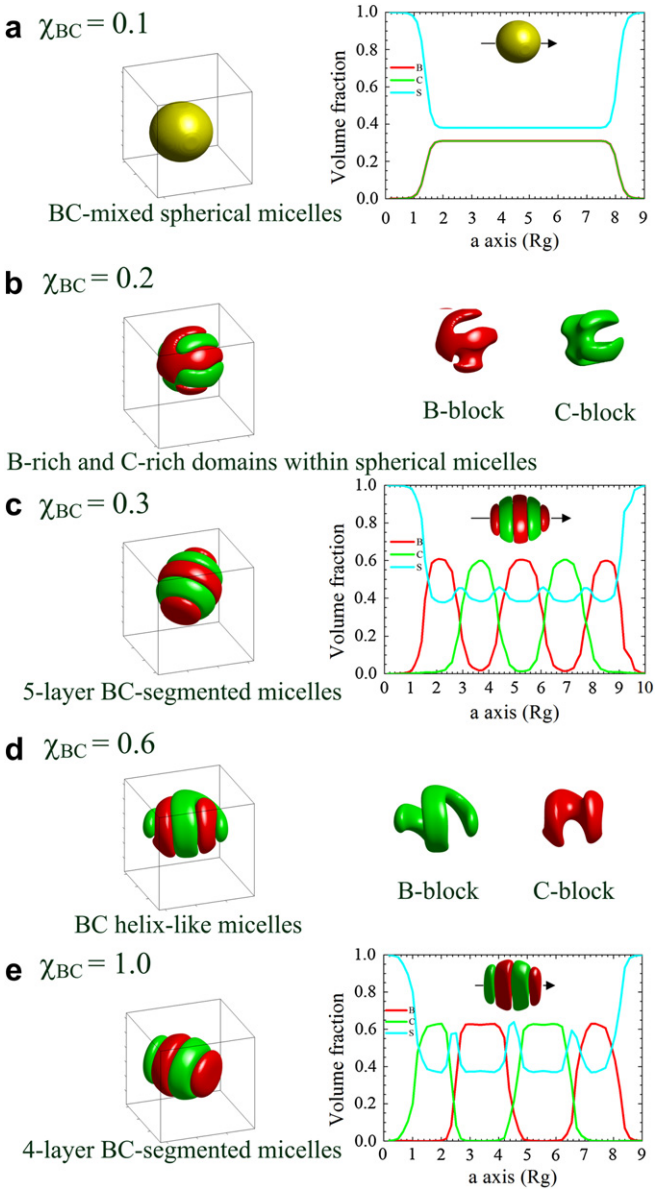

Fig. 4. Simulated micelle patterns and corresponding volume fraction profiles of B, C, and solvent S for BC diblock copolymers in a poor solvent with N = 120, ϕ = 0.1, $\chi_{BS} = \chi_{CS}$ = 0.9, and χ_{BC} equal to (a) 0.1, (b) 0.2, (c) 0.3, (d) 0.6, and (e) 1.0, respectively. In each representative of microstructures, B and C blocks are shown in light purple and green colors, respectively, and the solvent S is omitted for clarity. The BC-mixed is labeled as yellow. (For interpretation of the references to color in this figure legend, the reader is referred to the web version of this article.)

transitions is observed in Fig. 3: BC-mixed spherical micelles → BC-mixed ellipsoids → B-rich and C-rich domains within ellipsoids → 4-layer BC-segmented micelles. When the value of χ_{BC} parameter is small ($\chi_{BC} = 0.0-0.1$), as shown in Fig. 3a and b, the formed micelles are BC-mixed micelles as the neutral solvent can be served as a buffer region to reduce the incompatibility between B and C blocks. Therefore, the driving force at repulsive interactions χ_{BC} is not large enough for micelles to form the segregation of B and C blocks. However, it is interesting to note that the micelles are slightly elongated along the axis of the B and C blocks. The shape of micelles varies from spherical to ellipsoidal with the increasing of χ_{BC}. When the value of χ_{BC} parameter increases a little bit to 0.14 (Fig. 3c), the degree of incompatibility between B and C blocks will be sufficiently strong to form the small-length-scale segregation within the micelles. B and C blocks segregate into a two-phase B-rich and C-rich region, but there is no obvious orientation in the small-length-scale domain. When the value of χ_{BC} becomes greater than 0.2, B and C blocks form well-segregated domains within the micelles. The small-length-scale domain is packed with B and C alternating layers and thus they can have similar contact surface with solvent.

To understand the effect of χ_{BC} on the formation of micelles for BC diblock copolymers in a poor solvent, we decreased the incompatibility between the solvophobic blocks and solvent to be $\chi_{BS} = \chi_{CS} = 0.9$. The morphology transitions become different from those in the case of $\chi_{BS} = \chi_{CS} = 1.2$. A series of shape transitions are observed in Fig. 4: BC-mixed spherical micelles → B-rich and C-rich domains within spherical micelles → 5-layer BC-segmented micelles → BC helix-like micelles → 4-layer BC-segmented micelle. When the value of χ_{BC} is small ($\chi_{BC} = 0.0-0.1$), the micelles are always keeping the form of BC-mixed spherical micelles. From the profile of BC-mixed spherical micelles, shown in Fig. 4a, it can be found that the solvent aggregated within the micelles is more than that when $\chi_{BS} = \chi_{CS} = 1.2$. It shows that more solvent aggregated inside the micelles can release the osmotic pressure caused by the gradient of the solvent concentration inside and outside of the micelles. Therefore, the solvent effect on the shape of micelles becomes smaller when decreasing the value of $\chi_{BS} = \chi_{CS}$. When χ_{BC} value continuously increases to 0.3, B and C blocks are aggregated to form the segmented micelles. However, an interesting finding is the appearance of helix-like micelles in the transition of: segmented → helix-like → segmented. To explore what happens during the transition, we first discuss the variation of BC-segmented micelles as χ_{BC} value increases. Fig. 4c and e show the segmented morphologies formed by well-segregated B/C domains as well as the density profiles along the axis of the micelles. In the weak segregation conditions of $\chi_{BC} = 0.3-0.4$, the packing layers of BC-segmented micelles are found to be five. When χ_{BC} is larger than 1.0, however, the packing layers of segmented micelles are reduced to four to lessen the interfacial energy between B and C domains. The B/C helix-like micelles are formed between the five-layer and four-layer morphologies as an intermediate morphology when $\chi_{BC} = 0.6-0.8$. The reason is that the domain arrangement becomes highly frustrated when the domain layer deviates from the integer number. The formation of the B/C helix-like domains is thus an effective way to release the packing frustration.

The above discussions reveal that the shape of micelles is affected by the solvent quality. The phenomenon is analogous to the phase transitions of copolymers that are confined in a hard tube [63]. As compared with the hard confinement, it can be considered as a soft confinement that the shape variation of micelles occurs through tuning of the solvent quality for blocks. In a similar research, this matter was examined by Chi et al. [64]. They observed a transition in the shape of micelles of AB diblock copolymers from ellipsoidal to spherical with the increasing of the incompatibility between A block and solvent. In our simulations, we also discovered that the shape of copolymers can experience different transitions in the different solvent environments.

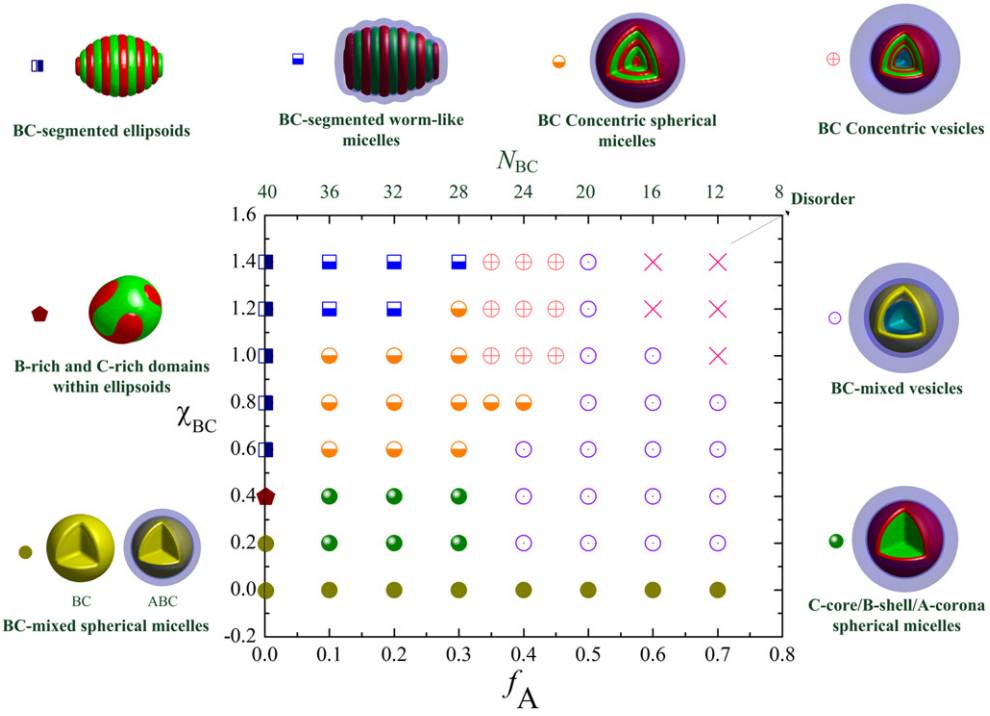

Fig. 5. The phase diagram of A-*b*-(B-*alt*-C)$_3$ multiblock terpolymers in dilute solutions in terms of χ_{BC} and f_A when $N = 120$, $\phi = 0.1$, $\chi_{AB} = \chi_{AC} = 1.0$, $\chi_{AS} = 0.27$, and $\chi_{BS} = \chi_{CS} = 1.2$. In each representative micelle, A, B, C, and S are shown in light purple, red, green, and light blue, respectively. The solvent S in the matrix is omitted for clarity. The BC-mixed is labeled as yellow. (For interpretation of the references to color in this figure legend, the reader is referred to the web version of this article.)

After examining the micelle formation of ABC and BC block copolymers, we turn to the investigation of the self-assembling behaviors of A-*b*-(B-*alt*-C)$_3$ multiblock terpolymer solutions in terms of f_A and χ_{BC}. The phase diagram when $N = 120$, $\phi = 0.1$, $\chi_{AB} = \chi_{AC} = 1.0$, $\chi_{AS} = 0.27$, and $\chi_{BS} = \chi_{CS} = 1.2$, is given in Fig. 5. First of all, we observed a variety of shape transitions with the increasing of χ_{BC} parameter. When f_A is in the range of small values (0.1–0.3), we observed a series of the morphology variations: BC-mixed spherical micelles → C-core/B-shell/C-corona spherical micelles → BC concentric spherical micelles → BC-segmented worm-like micelles, as shown in Fig. 6. In this case, the formed micelles are C-core/B-shell/A-corona spherical when the value of χ_{BC} is small (0.2–0.4). The shell is formed by B blocks because they join to A blocks. C blocks are curled into the core form. When increasing the χ_{BC} value, the shape of micelles is still spherical, but the number of shells increases in the small-length scale domains. The reason is that the segregation degree between B and C becomes strong enough to ensure each B and C blocks can be well segregated within the micelle. However, it is interesting to note that a shape transition of micelles occurs when χ_{BC} value is greater than 1.2. The micellar structure is transferred from spherical to worm-like. The B and C blocks are stacked by an alternating way. The orientation of the small-length scale domain becomes perpendicular to the shape of the micelles.

We also compared the BC-segmented worm-like micelles with the BC-segmented ellipsoids formed without solvophilic A block. Due to the protection from A block, each of B and C blocks is formed in disk shape to stack the cylindrical (worm-like) micelles. On the contrary, without the A block, the shape of micelles tends to form the ellipsoids, which have smaller surface areas than cylinders.

Next, we discussed the effect of f_A on the topology of the overall shape of micelles formed by the A-*b*-(B-*alt*-C)$_3$ multiblock terpolymers. As can be observed in Fig. 5, when χ_{BC} is weak so that B and C tend to mix together within the micelles, we observed the formation of BC-mixed spheres, independent of the f_A value. As χ_{BC}

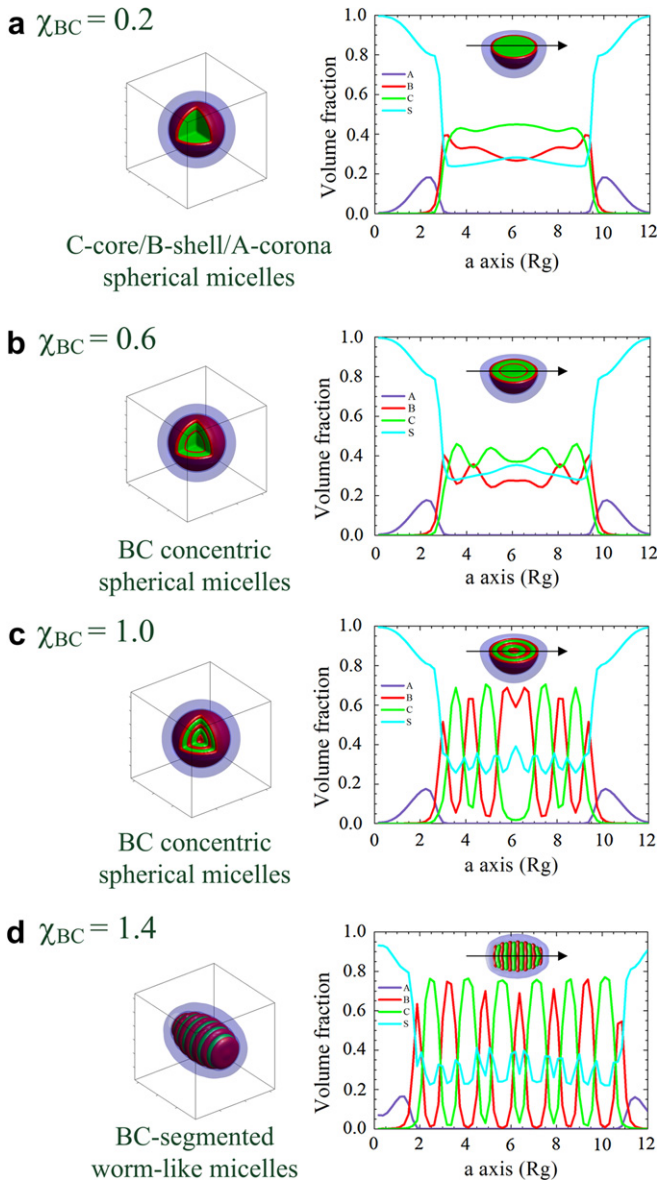

Fig. 6. Simulated micelle patterns and corresponding volume fraction profiles of A, B, C, and solvent S for A(BC)$_3$ multiblock terpolymers in a selective solvent for the A block when $N = 120$, $f_A = 0.3$, $\phi = 0.1$, $\chi_{AB} = \chi_{AC} = 1.0$, $\chi_{AS} = 0.27$, $\chi_{BS} = \chi_{CS} = 1.2$, and χ_{BC} is equal to (a) 0.2, (b) 0.6, (c) 1.0, and (d) 1.4, respectively. In each representative micelle, A, B, C, and S are shown in light purple, red, green, and light blue, respectively. The solvent S in the matrix is omitted for clarity. (For interpretation of the references to color in this figure legend, the reader is referred to the web version of this article.)

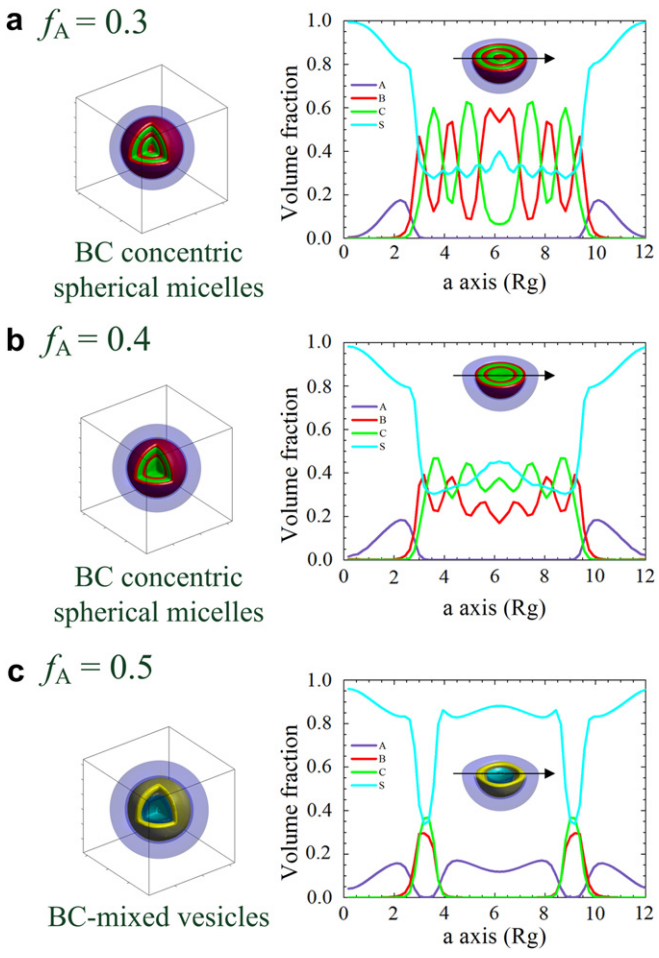

Fig. 7. Simulated micelle patterns and corresponding volume fraction profiles of A, B, C, and solvent S for A(BC)$_3$ multiblock terpolymers in a selective solvent for the A block when $N = 120$, $\phi = 0.1$, $\chi_{AB} = \chi_{AC} = 1.0$, $\chi_{AS} = 0.27$, $\chi_{BS} = \chi_{CS} = 1.2$, $\chi_{BC} = 0.8$, and f_A is equal to (a) 0.3, (b) 0.4, and (c) 0.5, respectively. In each representative micelle, A, B, C, and S are shown in light purple, red, green, and light blue, respectively. The solvent S in the matrix is omitted for clarity. The BC-mixed is labeled as yellow. (For interpretation of the references to color in this figure legend, the reader is referred to the web version of this article.)

increases to the range between 0.2 and 0.8, it is interesting to observe a transition from C core/B shell or BC concentric spherical micelles (f_A = 0.1–0.3) to BC-mixed vesicles (f_A = 0.4–0.7). This behavior is mainly attributed to the fact that the effective segregation between the alternating B and C blocks, $\chi_{BC}N_{BC}$, decreases with the increasing of f_A at a fixed degree of copolymerization N. Moreover, from the density profiles of all components along the diameter direction of microstructures plotted in Fig. 7a–c, where f_A = 0.3, 0.4, and 0.5, respectively, when χ_{BC} is fixed at 0.8, we observed a trend that more solvents are aggregated into the B and C segregated domains with an increase in f_A, and even can stay within the most inner core of micelles. As shown in Fig. 7c when f_A = 0.5, the inside hollow core is mostly aggregated by the solvent. The fact that the B and C blocks extremely dislike being in touch with the solvent enables a portion of the A blocks into the hollow core to protect the B and C blocks. Accordingly, our results have shown that the vesicles can be formed by the solvent-induced effect when the multiblock chains have a long solvophilic block. Fig. 8 shows the morphology variation and corresponding density profiles of all components with increasing f_A value when χ_{BC} = 1.0. A series of morphological transition from BC concentric spherical → BC concentric vesicles → BC-mixed vesicles → disorder state is observed. Although the result of this simulation is similar to that when χ_{BC} = 0.8, it is interesting to note that the multilayer vesicles are observed when f_A = 0.4. Recall that the vesicles have been commonly observed when the solvophilic A block is short in the AB diblock copolymers [65] or ABC triblock copolymers [37] due to the degree of corona-chain stretching. With a long solvophilic block, though the inside corona-chains are not easy to stretch freely within the vesicles, two types of BC-mixed and BC concentric multilayer vesicles can be formed by the solvent-induced effect.

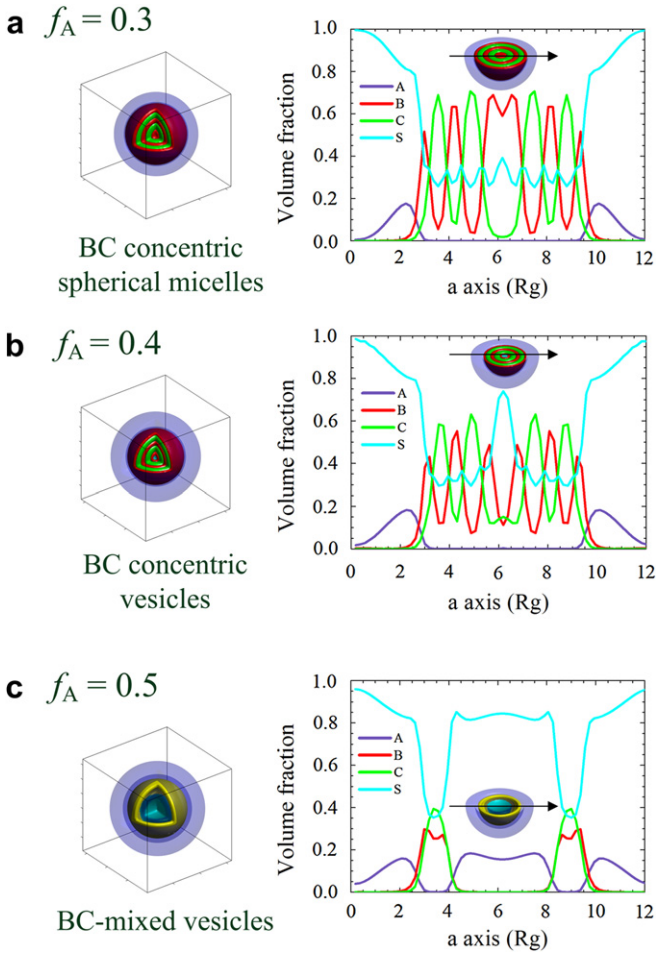

Fig. 8. Simulated micelle patterns and corresponding volume fraction profiles of A, B, C, and solvent S for A(BC)$_3$ multiblock terpolymers in a selective solvent for the A block when N = 120, ϕ = 0.1, $\chi_{AB} = \chi_{AC}$ = 1.0, χ_{AS} = 0.27, $\chi_{BS} = \chi_{CS}$ = 1.2, χ_{BC} = 1.0, and f_A is equal to (a) 0.3, (b) 0.4, and (c) 0.5, respectively. In each representative micelle, A, B, C, and S are shown in light purple, red, green, and light blue, respectively. The solvent S in the matrix is omitted for clarity. The BC-mixed is labeled as yellow. (For interpretation of the references to color in this figure legend, the reader is referred to the web version of this article.)

In the previous work [59], we examined the phase behavior of A$_2$-*star*-(B-*alt*-C)$_n$ multiblock terpolymers using the DPD simulation method. The results of the DPD simulation are usually doubted that the chain length is too short. When the multiblock terpolymer chains with a short solvophilic A block (f_A = 0.1–0.3) are in a neutral solvent for both solvophobic B and C blocks, the DPD simulation shows a transition from BC-mixed spherical micelles → B-rich and C-rich domains within spherical micelles → BC-segmented worm-like micelles with increasing the incompatibility degree between B and C. With an increase in f_A and a decrease in the number of repeating B and C blocks, n, the B–C–B hamburgers and helix-type micelles are favored. It is worthy to note that for the short ABC multiblocks to segregate within the micelles in a neutral poor solvent, the small-length-scale segregated layers only pack in a perpendicular direction with respect to the micelles. While, when considering the effect of polymer configurational entropy for long enough B and C alternating blocks, as in this current SCFT study, the internally B and C segregated domains can adopt both perpendicular and coaxial packings within the micelles, depending on both χ_{BC} and f_A. Even we can find the formation of BC-mixed and multilayer vesicles when the solvophilic A block becomes a majority component. Therefore, we discover more fascinating micelles by implementing the SCFT simulation than by the DPD simulation in the system of linear multiblock terpolymers. It shows that more chain stacking types can be performed in the SCFT simulations due to enhancing the effect of polymer configurational entropy.

4. Summary

We applied the three-dimensional SCFT method to examine the self-assembly behavior of A-*b*-(B-*alt*-C)$_n$ multiblock terpolymers in dilute solutions. The A block is solvophilic, whereas B and C are solvophobic. The phase diagrams of micelle morphology of ABC triblock terpolymers and A(BC)$_3$ multiblock terpolymers were constructed as a function of the incompatibility parameter between B and C, χ_{BC}, and the composition of the A block, f_A. In this work, we increased the degree of polymerization to 120, which is long enough to include the effect of polymer conformation entropy and thus more reasonable than that in the DPD simulations. We found that both χ_{BC} and f_A have a strong influence on the orientation of the small-length-scale B and C segregation within the micelles and thereafter the shape of micelles. With the increasing of χ_{BC} or decreasing of f_A, a segmented packing of B and C layers along the axial direction of the micelles is favored than the coaxial packing. Therefore, a variety of multicompartment micelle morphologies, such as core-shell-corona spherical micelles, hamburgers, and bump-surface micelles, have been observed. In the A(BC)$_3$ multiblock terpolymers, besides the BC-segmented worm-like micelles, which have been found in the DPD simulation work, we observed more types of micelles, such as concentric micelles and vesicles. That is because the small length of polymer chain definitely reduces the effect of polymer configurational entropy in the DPD simulation. Especially, the vesicles can be formed by the solvent-induced effect when the solvophilic block is a majority component. We also examined the influence of solvent quality on the micelle

morphology. By tuning the incompatibility for both the solvophobic blocks, we discovered the existence of helix-like micelles during the transition between 5-layer segmented and 4-layer segmented micelles. The SCFT method provides an efficient way to screen promising molecular architectures for the ability to self-assemble into technologically promising hierarchical structures.

Acknowledgments

This work was supported by the National Science Council of the Republic of China through grant NSC 100-2628-E-002-020-MY3. We also would like to thank the National Center for High-Performance Computing of Taiwan and the SHARCNET for the computing resources.

References

[1] Bates FS, Fredrickson GH. Annu Rev Phys Chem 1990;41(1):525–57.
[2] Smart T, Lomas H, Massignani M, Flores-Merino MV, Perez LR, Battaglia G. Nano Today 2008;3(3–4):38–46.
[3] Moughton AO, Hillmyer MA, Lodge TP. Macromolecules 2011;45(1):2–19.
[4] Freer EM, Krupp LE, Hinsberg WD, Rice PM, Hedrick JL, Cha JN, et al. Nano Lett 2005;5(10):2014–8.
[5] Park SM, Park OH, Cheng JY, Rettner CT, Kim HC. Nanotechnology 2008; 19(45):455304.
[6] Kataoka K, Harada A, Nagasaki Y. Adv Drug Deliver Rev 2001;47(1):113–31.
[7] Gaucher G, Dufresne MH, Sant VP, Kang N, Maysinger D, Leroux JC. J Control Release 2005;109(1–3):169–88.
[8] Segalman RA, McCulloch B, Kirmayer S, Urban JJ. Macromolecules 2009; 42(23):9205–16.
[9] Sommer M, Huettner S, Thelakkat M. J Mater Chem 2010;20(48):10788–97.
[10] Matsen MW, Schick M. Phys Rev Lett 1994;72(16):2660–3.
[11] Matsen MW. J Phys Condens Matter 2002;14(2):R21–47.
[12] Tyler CA, Morse DC. Phys Rev Lett 2005;94(20):208302.
[13] Tang P, Qiu F, Zhang HD, Yang YL. Phy Rev E 2004;69(3):031803.
[14] Tang P, Qiu F, Zhang HD, Yang YL. J Phys Chem B 2004;108(24):8434–8.
[15] Ye XG, Shi TF, Lu ZY, Zhang CX, Sun ZY. Macromolecules 2005;38(21):8853–7.
[16] Tyler CA, Qin J, Bates FS, Morse DC. Macromolecules 2007;40(13):4654–68.
[17] Guo ZJ, Zhang GJ, Qiu F, Zhang HD, Yang YL, Shi AC. Phys Rev Lett 2008;101(2): 028301.
[18] Huang CI, Fang HK, Lin CH. Phys Rev E 2008;77(3):031804.
[19] Stadler R, Auschra C, Beckmann J, Krappe U, Voigtmartin I, Leibler L. Macromolecules 1995;28(9):3080–97.
[20] Balsamo V, von Gyldenfeldt F, Stadler R. Macromolecules 1999;32(4):1226–32.
[21] Nagata Y, Masuda J, Noro A, Cho DY, Takano A, Matsushita Y. Macromolecules 2005;38(24):10220–5.
[22] Masuda J, Takano A, Nagata Y, Noro A, Matsushita Y. Phys Rev Lett 2006;97(9): 098301.
[23] Masuda J, Takano A, Suzuki J, Nagata Y, Noro A, Hayashida K, et al. Macromolecules 2007;40(11):4023–7.
[24] Fleury G, Bates FS. Macromolecules 2009;42(5):1691–4.
[25] Fleury G, Bates FS. Macromolecules 2009;42(10):3598–610.
[26] Alfonzo CG, Fleury G, Chaffin KA, Bates FS. Macromolecules 2010;43(12): 5295–305.
[27] Faber M, Voet VSD, ten Brinke G, Loos K. Soft Matter 2012;8(16):4479–85.
[28] Nap R, Erukhimovich I, ten Brinke G. Macromolecules 2004;37(11):4296–303.
[29] Nap R, Sushko N, Erukhimovich I, ten Brinke G. Macromolecules 2006;39(19): 6765–70.
[30] Subbotin A, Klymko T, ten Brinke G. Macromolecules 2007;40(8):2915–8.
[31] Klymko T, Subbotin A, ten Brinke G. J Chem Phys 2008;129(11):114902.
[32] Huang CI, Chen CM. ChemPhysChem 2007;8(18):2588–94.
[33] Li WH, Shi AC. Macromolecules 2009;42(3):811–9.
[34] Xu YC, Li WH, Qiu F, Yang YL, Shi AC. Phys Chem Chem Phys 2011;13(27): 12421–8.
[35] Xu Y, Li WH, Qiu F, Yang YL, Shi AC. J Phys Chem B 2010;114(46):14875–83.
[36] Wang LQ, Lin JP, Zhang L. Macromolecules 2010;43(3):1602–9.
[37] Yu GE, Eisenberg A. Macromolecules 1998;31(16):5546–9.
[38] Talingting MR, Munk P, Webber SE, Tuzar Z. Macromolecules 1999;32(5): 1593–601.
[39] Gohy JF, Willet N, Varshney S, Zhang JX, Jerome R. Angew Chem Int Ed 2001; 40(17):3214–6.
[40] Kubowicz S, Baussard JF, Lutz JF, Thunemann AF, von Berlepsch H, Laschewsky A. Angew Chem Int Ed 2005;44(33):5262–5.
[41] Hu J, Njikang G, Liu G. Macromolecules 2008;41(21):7993–9.
[42] Skrabania K, Laschewsky A, von Berlepsch H, Boettcher C. Langmuir 2009; 25(13):7594–601.
[43] Jiang X, Zhang G, Narain R, Liu S. Langmuir 2009;25(4):2046–54.
[44] Skrabania K, von Berlepsch H, Boettcher C, Laschewsky A. Macromolecules 2010;43(1):271–81.
[45] Walther A, Barner-Kowollik C, Mueller AHE. Langmuir 2010;26(14): 12237–46.
[46] Erhardt R, Zhang MF, Boker A, Zettl H, Abetz C, Frederik P, et al. J Am Chem Soc 2003;125(11):3260–7.
[47] Liu YF, Abetz V, Muller AHE. Macromolecules 2003;36(21):7894–8.
[48] Laschewsky A. Curr Opin Colloid Interface Sci 2003;8(3):274–81.
[49] Thünemann AF, Kubowicz S, von Berlepsch H, Mohwald H. Langmuir 2006; 22(6):2506–10.
[50] Beheshti N, Zhu K, Kjoniksen A-L, Knudsen KD, Nystrom B. Soft Matter 2011; 7(3):1168–75.
[51] Ren T, Lei X, Yuan W. Mater Lett 2012;67(1):383–6.
[52] Fredrickson GH. The equilibrium theory of inhomogeneous polymers. Oxford: Oxford University Press; 2006. p. 203–79.
[53] Chou SH, Tsao HK, Sheng YJ. J Chem Phys 2006;125(19):194903.
[54] Zhu Y, Yu H, Wang Y, Cui J, Kong W, Jiang W. Soft Matter 2012;8(17): 4695–707.
[55] Wang R, Tang P, Qiu F, Yang YL. J Phys Chem B 2005;109(36):17120–7.
[56] Ma ZW, Jiang W. J Polym Sci Part B Polym Phys 2009;47(5):484–92.
[57] Ma ZW, Yu HZ, Jiang W. J Phys Chem B 2009;113(11):3333–8.
[58] Wang LQ, Lin JP. Soft Matter 2011;7(7):3383–91.
[59] Huang CI, Liao CH, Lodge TP. Soft Matter 2011;7(12):5638–47.
[60] Drolet F, Fredrickson GH. Phys Rev Lett 1999;83(21):4317–20.
[61] Drolet F, Fredrickson GH. Macromolecules 2001;34(15):5317–24.
[62] Tzeremes G, Rasmussen KO, Lookman T, Saxena A. Phys Rev E 2002;65(4): 041806.
[63] Suo TC, Yan DD. Polymer 2011;52(7):1686–91.
[64] Chi P, Wang Z, Li BH, Shi AC. Langmuir 2011;27(18):11683–9.
[65] Zhang LF, Eisenberg A. J Am Chem Soc 1996;118(13):3168–81.